

Effect of Hydrolyzing Agents on the Properties of Poly (Ethylene Glycol)-Fe₃O₄ Nanocomposite

E. Karaoğlu^{1,*}, H. Kavas², A. Baykal¹, M. S. Toprak³, H. Sözeri⁴

(Received 28 April 2011; accepted 15 June 2011; published online 23 June 2011.)

Abstract: Poly (ethylene glycol) (PEG) assisted hydrothermal route has been used to study the influence of the hydrolyzing agent on the properties of PEG-iron oxide (Fe₃O₄) nanocomposites. Iron oxide nanoparticles (NPs), as confirmed by X-ray diffraction analysis, have been synthesized by a hydrothermal method in which NaOH and NH₃ were used as hydrolyzing agents. Formation of PEG-Fe₃O₄ nanocomposite was confirmed by Fourier transform infrared spectroscopy (FTIR). Samples exhibit different crystallite sizes, which estimated based on line profile fitting as 10 nm for NH₃ and 8 nm for NaOH hydrolyzed samples. The average particle sizes obtained from transmission electron microscopy was respectively 174±3 nm for NaOH and 165±4 nm for NH₃ gas hydrolyzed samples. Magnetic characterization results reveal superparamagnetic characteristics despite a large particle size, which indicate the absence of coupling between the nanocrystals due to the presence of polymer in the nanocomposites. The conductivity curve demonstrates that σ_{DC} is strongly temperature dependent.

Keywords: Magnetite; PEG; Hydrothermal synthesis; Conductivity; Magnetization

Citation: E. Karaoğlu, H. Kavas, A. Baykal, M. S. Toprak and H. Sözeri, "Effect of Hydrolyzing Agents on the Properties of Poly (Ethylene Glycol)-Fe₃O₄ Nanocomposite", Nano-Micro Lett. 3 (2), 79-85 (2011). <http://dx.doi.org/10.3786/nml.v3i2.p79-85>

Introduction

Magnetic particles have been widely studied because of their fascinating properties and wide range of potential applications in ferrofluids, information storage and medicine. Among magnetic particles, iron oxides (Fe₂O₃ and Fe₃O₄) have been extensively investigated [1-3]. The intrinsic properties of these particles are mainly determined by its size, shape, composition, crystallinity and structure [4-6].

Over the past decade, the Fe₃O₄ has been widely used in many applications such as magnetic recording, ferrofluids, magnetic separation, magnetic resonance imaging, and catalysis for a long time [7-12]. When the particle size of Fe₃O₄ is decreased to nanoscales,

it exhibits superparamagnetic behavior [13,14]. This nanosize effect together with biocompatible properties of the material are considered of great potential for applications in biotechnology and biomedicine including bio-assays, magnetic resonance imaging (MRI), magnetically guided drug delivery, and hyperthermia [15-17].

Meanwhile, in bio-nanotechnology, the biocompatibility of most nanoparticles could be greatly improved by introduce poly(ethylene glycol) (PEG) to their surface. In general, attachment of PEG promotes water solubility, reduces toxicity, decreases enzymatic degradation, and increases the in vivo half-lives of small-molecule drugs [18]. PEG has frequently been used as a soft template for building 1D nanostructures due to its long-chain structure and selective absorption on

¹Department of Chemistry^b, Fatih University, 34500, B.Cekmece-Istanbul/TURKEY

²Department of Physics, Gebze Institute of Technology, 41400, Cayirova-Izmit/TURKEY

³Functional Materials Division, Royal Institute of Technology - KTH, SE16440 Stockholm, Sweden

⁴TUBITAK-UME, National Metrology Institute, PO Box 54, 41470, Gebze-Kocaeli/TURKEY

*Corresponding author. E-mail: ekaraoglu@fatih.edu.tr

preferred facets [19]. PEG with adsorbed by magnetic nanoparticles can prolong circulation time in a bloodstream. The modification of magnetite nanoparticles with PEG could be used to resist the protein adsorption and thus avoid their recognition by macrophage cells and simultaneously facilitate the nanoparticles uptake to specify cancer cells in a cancer therapy [20,21].

Size-controlled Fe_3O_4 nanoparticles were prepared via a facile solvothermal method by using mixed surfactants of SDS and PEG as protective reagents by Liu et al. [22]. They found that the mixture of SDS and PEG could act as a more efficient protective reagent than SDS or PEG alone. Quasi-hexagonal $\alpha\text{-Fe}_2\text{O}_3$ nanoplates with lateral sizes of 40~60 nm and thickness of ca. 10 nm were fabricated by a facile poly (ethylene glycol 600) (PEG-600) assisted hydrothermal technique in combination with calcination method by Zhang et al. [23]. Zhen et al. [24] studied the PEG (Mwt = 400, 1000, 20,000) assisted hydrothermal synthesis of single-crystalline Fe_3O_4 nanowires. Dong et al. [25] synthesized the Fe_3O_4 nanoparticles via a simple technique at room temperature using PEG as a template.

Here, we report the synthesis of PEG- Fe_3O_4 nanocomposite. This is, to date, the first report using the adopted route for the synthesis of a PEG- Fe_3O_4 nanocomposite. Comprehensive physicochemical and magnetic characterization results are presented.

Experimental

Chemicals and Instrumentation

All chemicals, including $\text{FeCl}_3 \cdot 6\text{H}_2\text{O}$ (99%), $\text{FeCl}_2 \cdot 4\text{H}_2\text{O}$ (99%), NaOH PEG-400 (99%), and NH_3 gas (From HABAS, Turkey), were purchased from Merck and used as received without further purification.

X-ray powder diffraction (XRD) analysis was conducted on a Rigaku Smart Lab Diffractometer operated at 40 kV and 35 mA using $\text{Cu K}\alpha_1$.

Fourier transform infrared (FTIR) spectra of the samples were measured with a Perkin Elmer BX FT-IR infrared spectrometer in the range of 400~4000 cm^{-1} .

Transmission electron microscopy (TEM) analysis was performed using a FEI Tecnai G2 Sphera microscope. A drop of diluted sample in alcohol was dripped on a TEM grid. Particle size distribution was obtained from several micrographs, counting a number of minimum of 150 particles.

Thermal stability was determined by thermogravimetric analysis (TGA, Perkin Elmer Instruments model, STA 6000). TGA thermograms were measured for 5 mg of powder sample at a heating rate of 10°C/min in the temperature range of 30°C~700°C under nitrogen atmosphere.

Electrical conductivity of the PEG- Fe_3O_4 has been

studied in the range of 20~120°C with 10°C increment steps. The samples were used in the form of circular pellets with 13 mm diameter and 3 mm thickness. The pellets were sandwiched between gold electrodes and the conductivities were measured using Novocontrol dielectric impedance analyzer in the frequency range 1 Hz to 3 MHz. The temperature was controlled by a Novocool Cryosystem, between -100°C to 250°C. The dielectric data (ϵ' and ϵ'') were collected during heating as a function of frequency.

Room temperature VSM measurements have been conducted by using a quantum design vibrating sample magnetometer (QD-VSM).

Procedure

a) Synthesis of Fe_3O_4 NPs and PEG- Fe_3O_4 nanocomposite

In a typical experiment, 2.79 g of $\text{FeCl}_3 \cdot 6\text{H}_2\text{O}$ and 1 g of $\text{FeCl}_2 \cdot 4\text{H}_2\text{O}$ were added dropwise into a separate 50 ml two separate Teflon-lined stainless autoclaves, then 30 ml PEG-400, heated and melted, was injected to each autoclave. The hydrolysis was performed by the addition of 1M NaOH solution (TE2) for the first autoclave and NH_3 gas (TE1) for the second until the pH of each solution is equal to 11. After continuous stirring, homogeneous solutions were obtained. The autoclaves were kept at 160°C for 12 h, then cooled to room temperature. The products were filtered and washed several times with distilled water and absolute ethanol, and finally dried in a vacuum oven at 50°C for 12 h.

Results and Discussion

XRD Analysis

Phase investigation of the crystalline products has been conducted using XRD and the patterns are presented in Fig. 1. The XRD patterns indicate that the products were iron oxide, Fe_3O_4 , and broadening of the diffraction peaks were observed owing to the small crystallite size. All the observed diffraction peaks could be indexed by the cubic structure of Fe_3O_4 (JCPDS no 19-629) indicating a high phase purity of iron oxide. The mean size of the crystallites was estimated from the diffraction pattern by line profile fitting method using the equation (1) given in Ref 26, and 27 (equation given below). The line profile, shown in Fig. 1, were fitted for observed seven peaks with the following miller indices: (111), (220), (311), (400), (422), (511), (440). The average crystallite size, D and σ , was obtained as 10 ± 2 nm and 8 ± 2 nm for TE1 and TE2 samples, respectively, as the result of this line profile fitting.

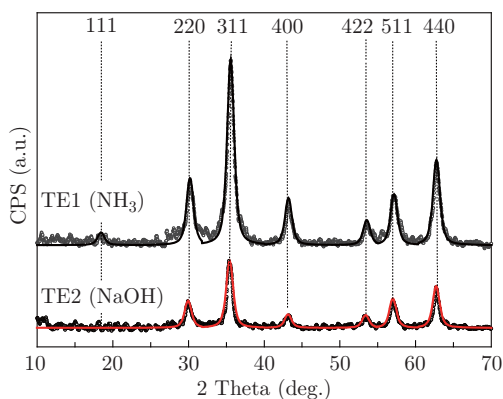


Fig. 1 XRD powder patterns of TE1 and TE2 samples.

FT-IR Analysis

FTIR spectra of as synthesized PEG-Fe₃O₄ nanocomposites by using NaOH (TE2) and NH₃ (TE1) as hydrolyzing agent; TE1 and TE2 are shown in Fig. 2. As prepared powder presents characteristic peaks of magnetite powder: metal-oxygen band, observed at ν_1 (590 cm⁻¹) corresponds to intrinsic stretching vibrations of the metal at tetrahedral site (Fe_{tetra} ↔ O), whereas metal-oxygen band observed at ν_2 (445 cm⁻¹) is assigned to octahedral-metal stretching (Fe_{octa} ↔ O) [28-33]. The FT-IR measurements reveal that the vibration band of C-O bond shifts from 1113 cm⁻¹ for pure ethylene glycol to 1095 cm⁻¹ for the nanocomposite which indicates that the O from C-O coordinates Fe on the surface of Fe₃O₄ NP's. The presence of C-O (~1106 cm⁻¹), -CH₂ (~2900 cm⁻¹) and -CH (~2800 cm⁻¹) peaks were strong evidence that PEG was chemically bonded to the surface of nanoparticles. The surfactant molecules in the adsorbed state are influenced by the field of solid-state surface. As a result, the characteristic bands shifted to a lower frequency region. In the previous reports [34-38], it has been concluded that the functional head groups of the surfactant have coordination bond or strong interaction with nanoparticles, and thus kinetically control the growth rates of various faces of crystals, which can control the morphology. As a surfactant, PEG is one of the polymers with major interest in this area because it is nontoxic, nonflammable and easy to handle. The PEG with a uniform and ordered chain structure is easily adsorbed at the surface of metal oxide colloid has been reported. When the surface of the colloid adsorbs this type of polymer, the activities of colloid will greatly decrease and the growth rate of the colloids in some certain facet will be confined [39,40]. Therefore, the addition of PEG in the reaction system will modify the kinetics of the growth process, which leads to anisotropic growth of the crystal. Linear PEG used in the synthesis of series of nanoparticles and 1D material in solution [40].

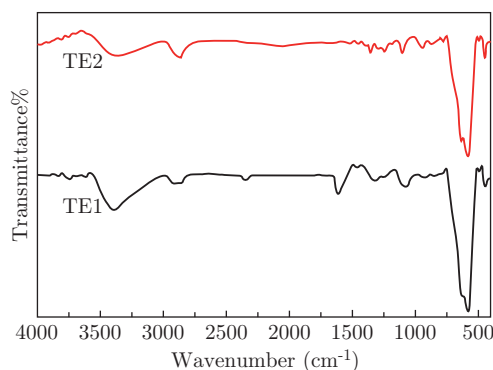


Fig. 2 FTIR spectra of TE1 and TE2 samples.

TEM Analysis

TEM analysis performed to investigate the morphology of the PEG-Fe₃O₄ nanocomposites. Micrographs and size distribution histograms calculated thereof are presented in Fig. 3(a) and 3(b). Fe₃O₄ particles observed to have more edgy morphology including squares, polygons and parallelograms; particles also agglomerated. It is most likely due to the influence of the chemisorbed PEG on the growth of nanoparticles and eventually sticking/clustering particles together. Size distribution histogram is obtained by measuring at least 150 nanoparticles and is fitted by using a log-normal function as follows [41].

An average size, $D_{TEM/log-normal}$, of 173±3 nm and 165±4 nm was obtained for magnetite nanoparticles in TE2 and TE1 nanocomposites, respectively. Crystallite size obtained from XRD line profile fitting vs. particle size estimated from TEM, reveal the polycrystalline characteristics of observed particles.

Thermal analysis

Thermal stability of the precursor and final powders is analyzed by using TGA. To confirm the existence of PEG on the surface of Fe₃O₄ NPs and quantify the proportion of organic and inorganic phases, TGA was measured in the temperature range of 30~700°C and the thermograms are presented in Fig. 4. Pure PEG (as shown in Fig. 4c) combustion started at ~340°C and completely combusted at ~420°C [42]. PEG-400 shows approximately 100% weight loss in the 30~700°C temperature range of TG analysis. Degradation of PEG over the iron oxide begins at a much lower temperature. This behavior could originate from the fact that iron oxide particles behave as catalysts thus reducing the degradation temperature of PEG. Moreover, temperature range between degradation onset and offset points on the DTG curves for PEG is wider than that for the nanocomposite. This result might also be attributed to catalytic effects of nanoparticles for the degradation of PEG [43,44]. TE1 and TE2 nanocomposites (as shown in Fig. 4a and 4b) show a major weight loss of 16% and

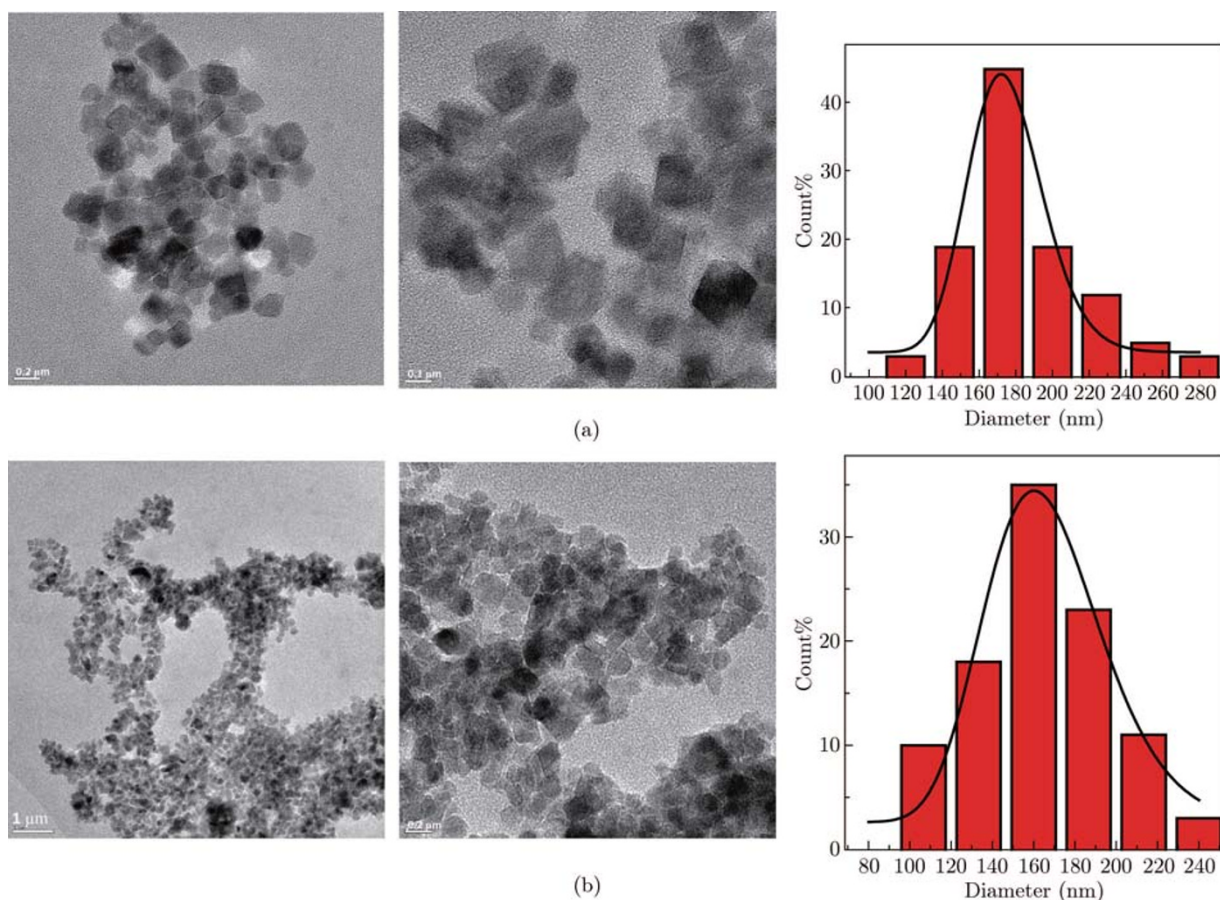


Fig. 3 TEM micrographs and size distribution histograms (with log-normal fitting) of (a) TE2 and (b) TE1 samples.

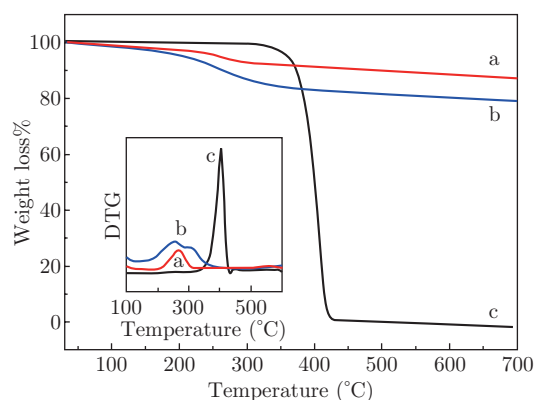


Fig. 4 TGA thermograms of (a) TE1, (b) TE2 and (c) PEG.

22% over the temperature range of 30~700°C due to the decomposition and combustion of PEG respectively. These results imply that TE1 nanocomposite has 84% inorganic phase (Fe_3O_4) and TE2 nanocomposite has around 78% inorganic phase.

Magnetization

Under room temperature, M-H hysteresis curves of PEG- Fe_3O_4 nanocomposites measured up to 1.5 T are shown in Fig. 5. It reveals that magnetization curves

are immeasurable coercively and remanence. Consequently, they do not show a hysteretic behavior. Besides, magnetization increases with external magnetic field strength, however, it does not reach to saturation even at 1.5 T. These observed properties are all typical features of superparamagnetic (SP) nanoparticles. Saturation magnetization (M_s) values of the nanocomposites are calculated from a plot of M vs. $1/H$ (M at $1/H \geq 0$) as 54.6, 51.9 and 64 emu/g for TE1, TE2 and bulk Fe_3O_4 , respectively, and appeared considerably lower than that of the bulk magnetite (92 emu/g) [45]. Here, we should notice that overall weight of the nanocomposites include the sum of the masses of magnetite and PEG coating. If we normalize these magnetization values to the mass of the magnetite only, derived from the TGA analysis in Fig. 3, M_s of sample TE2 becomes 59.5 emu/g and 69.3 emu/g of TE1, which are still lower than the theoretical M_s of bulk magnetization. However, reduced magnetization is generally observed in SP magnetite particles [32,45-48]. In the literature, the low magnetization values of SP particles can be explained by the spin canting and the presence of disordered spins at the surface [49]. As particle size decreases, effect of surface spins to the overall magnetization increases due to the presence of a considerably

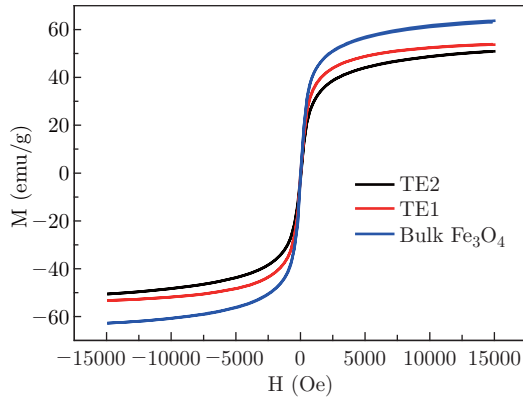


Fig. 5 Magnetization versus applied field at room temperature for TE1, TE2 samples and bulk Fe_3O_4 .

high fraction of all spins on the surface. For instance, half of the overall spins can lie on the surface of the nanoparticles [49,50]. In addition to spin canting and presence of disordered spins at the surface, adsorption of surfactant molecules to the surface of magnetite particles can be another reason of low magnetization values in the nanocomposites. In general, we have observed in our previous works [32,48,51] as well as in this study also, that surfactant molecules are bound to the surface via oxygen atoms as revealed from FTIR data. As a result, some of the spins of the oxygen atoms close to the surface are pinned which weak the super exchange

interaction between Fe-O-Fe atoms. Then, overall magnetization of the nanocomposite decreases.

Room temperature magnetization curves can be used to calculate average particle size of the nanocomposites with an assumption that they are weakly- or non-interacting SP particles. Magnetization of these particles can be described by the Langevin function which should be fit to the experimental data. Then, mean magnetic moment (μ) of particles is found to determine average particle size (D). Accordingly, mean magnetic moments of TE1 and TE2 samples with normalized masses are calculated as $10.621 \mu_B$ and, $7.743 \mu_B$ respectively. When these values are inserted in $\mu = M_s \pi \rho D^3 / 6$, where ρ is the density of the magnetite particles $\approx 5.18 \text{ g/cm}^3$, average particle sizes are found to be $8.2 \pm 2 \text{ nm}$ and $7.7 \pm 2 \text{ nm}$ for the samples TE1 and TE2, respectively, and agrees with the crystallite sizes determined from XRD powder patterns.

Temperature and frequency dependent conductivity and dielectric permittivity measurements

The AC conductivity (σ_{AC}) curves of TE1 and TE2 samples as shown in Fig. 6. The σ_{AC} is generally increasing with increasing temperature and frequency. The σ_{AC} does not change so much with frequency at low temperatures but at higher temperatures, it increases exponentially with increasing temperature.

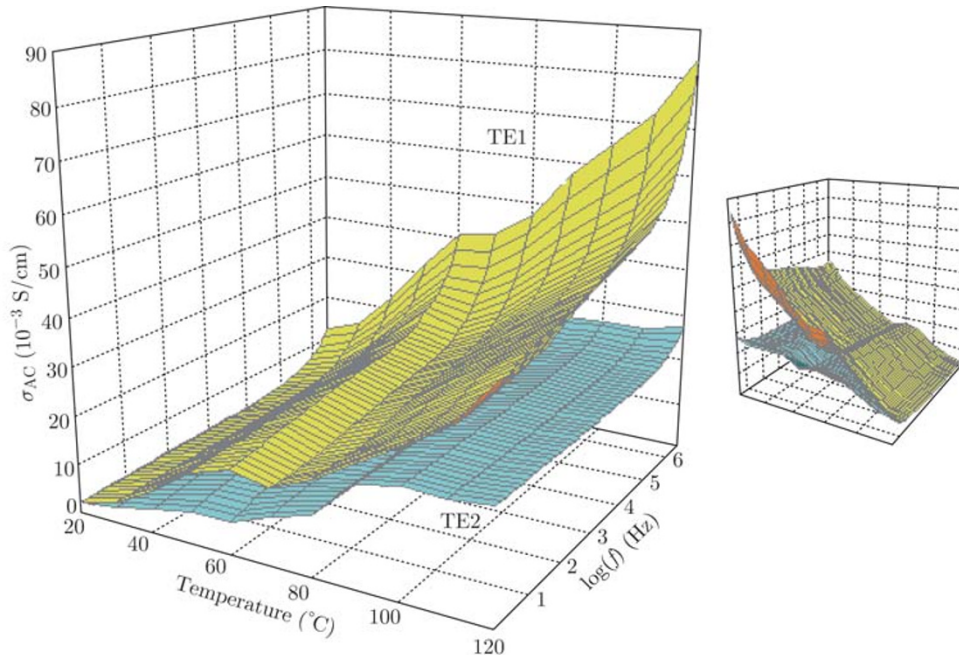


Fig. 6 The σ_{AC} versus $\log(f)$ and temperature surface for TE1 and TE2 samples (The inset shows the view in the opposite direction).

The σ_{DC} conductivity of the TE1 and TE2 nanocomposites investigate from the frequency independent part of σ_{AC} curves and obtained curves are demonstrated

in Fig. 7. The conductivity curve demonstrates that σ_{DC} strongly depends on temperature. These σ_{DC} curves are fitted with Arrhenius equation as $\sigma_{dc} =$

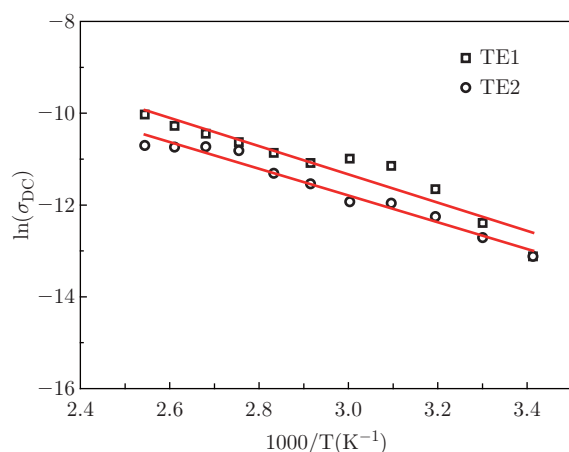


Fig. 7 DC conductivity of PEG-Fe₃O₄ nanocomposites TE1 and TE2 samples versus reciprocal temperature.

$\sigma_0 \exp(-\frac{E_a}{k_B T})$ and the activation energies of $E_a = 0.251$ eV and 0.265 eV are found for TE1 and TE2, respectively. These results are comparable with the E_a of Carnosine coated Fe₃O₄ (0.312 eV) [30] and that of Alginate-coated Fe₃O₄ nanocomposite (0.151) [31].

Conclusion

In this investigation, iron oxide (Fe₃O₄) nanoparticles have been successfully synthesized by a PEG-assisted hydrothermal method in which NaOH and NH₃ gas were used as hydrolyzing agents. Formation of PEG-Fe₃O₄ nanocomposites are confirmed by XRD and FTIR analysis. Samples exhibit different crystallite sizes, estimated based on line profile fitting as 10 nm for NaOH and 8 nm for NH₃ gas hydrolyzed samples. Average particle sizes, obtained from TEM analysis as 174±3 nm for NaOH and 165±4 nm for NH₃ gas hydrolyzed samples, indicate clearly that particles are polycrystalline. Magnetic characterization results reveal superparamagnetic character despite a large particle size, and magnetic domain size is estimated to be in the order of 8 nm for both samples, which evidence multi-domain character of the observed particles and the absence of coupling between the nanocrystals due to the presence of polymer in the nanocomposite. The conductivity curve demonstrates that σ_{DC} strongly depends on the temperature. Since many intrinsic properties of magnetic nanoparticles are size-dependent, we believe that these nanoparticles with different sizes will have important applications not only in advanced magnetic materials and ferrofluid technology, but also in biomedical applications such as biomolecular separations, targeted drug delivery, cancer diagnosis and treatment, as well as magnetic resonance imaging. In addition, Fe₃O₄/PEG nanocomposite can also be

used as thermoseeds for localized hyperthermia treatment of cancers.

Acknowledgements

The authors are thankful to the Fatih University, Research Project Foundation (Contract no: P50020902-2), Scientific and Technological Research Council of Turkey (TÜBİTAK) (Project no:110T487).

References

- [1] W. Weiss and W. Ranke, *Prog. Surf. Sci.* 70, 1 (2002). [http://dx.doi.org/10.1016/S0079-6816\(01\)00056-9](http://dx.doi.org/10.1016/S0079-6816(01)00056-9)
- [2] M. K. Krause, M. Ziese, R. Hohne, A. Pan, A. Galkin and E. Zeldov, *J. Magn. Magn. Mater.* 1097, 242 (2002).
- [3] D. Beydoun, R. Amal, G. K. C. Low and S. McEvoy, *J. Phys. Chem. B* 104, 4387 (2000). <http://dx.doi.org/10.1021/jp992088c>
- [4] V. F. Puentes, K. M. Krishnan and A. P. Alivisatos, *Science* 291, 2115 (2001). <http://dx.doi.org/10.1126/science.1057553>
- [5] C. M. Lieber, *Solid State Commun.* 107, 607 (1998). [http://dx.doi.org/10.1016/S0038-1098\(98\)00209-9](http://dx.doi.org/10.1016/S0038-1098(98)00209-9)
- [6] Z. W. Pan, Z. R. Dai and Z. L. Wang, *Science* 291, 1947 (2001). <http://dx.doi.org/10.1126/science.1058120>
- [7] K. Yamaguchi, K. Matsumoto and T. Fujii, *J. Appl. Phys.* 67, 4493 (1990). <http://dx.doi.org/10.1063/1.344892>
- [8] R. Kaiser and G. Miskolcze, *J. Appl. Phys.* 41, 1064 (1970). <http://dx.doi.org/10.1063/1.1658812>
- [9] Z. M. Saiyed, M. Parasramka, S. D. Telang and C. N. Ramchand, *Anal. Biochem.* 363, 288 (2007). <http://dx.doi.org/10.1016/j.ab.2007.01.008>
- [10] A. K. Gupta and M. Gupta, *Biomaterials* 26, 3995 (2005). <http://dx.doi.org/10.1016/j.biomaterials.2004.10.012>
- [11] S. Guo, D. Li, L. Zhang, J. Li and E. Wang, *Biomaterials* 30, 1881 (2009). <http://dx.doi.org/10.1016/j.biomaterials.2008.12.042>
- [12] D. H. Zhang, G. D. Li, J. X. Li and J. S. Chen, *Chem. Commun.* 29, 3414 (2008). <http://dx.doi.org/10.1039/b805737k>
- [13] G. F. Goya, T. S. Berquo and F. C. Fonseca, *J. Appl. Phys.* 94, 3520 (2003). <http://dx.doi.org/10.1063/1.1599959>
- [14] A. Angermann and J. Töpfer, *J. Mater. Sci.* 43, 5123 (2008). <http://dx.doi.org/10.1007/s10853-008-2738-3>
- [15] P. Majewski and B. Thierry, *Crit. Rev. Solid State Mater. Sci.* 32, 203 (2007). <http://dx.doi.org/10.1080/10408430701776680>
- [16] Y. Lin and C. Haynes, *Chem. Mater.* 21, 3979 (2009). <http://dx.doi.org/10.1021/cm901259n>

- [17] R. Hao , R. Xing , Z. Xu , Y. Hou, S. Gao and S. Sun, *Adv. Mater.* 22, 2729 (2010). <http://dx.doi.org/10.1002/adma.201000260>
- [18] L. Xu, M. J. Kim, K. D. Kim, Y. H. Choa and H. T. Kim, *Colloid. Surface. A* 350, 8 (2009). <http://dx.doi.org/10.1016/j.colsurfa.2009.08.022>
- [19] Z. B. Huang, Y. Q. Zhang and F. Q. Tang, *Chem. Commun.* 3, 342 (2005). <http://dx.doi.org/10.1039/b410463c>
- [20] A. Jozefczak and A. Skumiel, *J. Magn. Magn. Mater.* 323, 1509 (2011). <http://dx.doi.org/10.1016/j.jmmm.2011.01.009>
- [21] Y. Zhang, N. Kohler and M. Zhang, *Biomaterials* 23, 1553 (2002). [http://dx.doi.org/10.1016/S0142-9612\(01\)00267-8](http://dx.doi.org/10.1016/S0142-9612(01)00267-8)
- [22] A. G. Yan, X. Liu, G. Qiu, H. Wu, R. Yi, N. Zhang and J. Xu, *J. Alloy. Compd.* 458, 487 (2008). <http://dx.doi.org/10.1016/j.jallcom.2007.04.019>
- [23] G. Y. Zhang, Y. Y. Xu, D. Z. Gao and Y. Q. Sun, *J. Alloy. Compd.* 509, 885 (2011). <http://dx.doi.org/10.1016/j.jallcom.2010.09.124>
- [24] K. He, C. Y. Xu, L. Zhen and W. Z. Shao, *Mater. Lett.* 61, 3159 (2007). <http://dx.doi.org/10.1016/j.matlet.2006.11.023>
- [25] Y. Y. Zheng, X. B. Wang, L. Shang, C. R. Li, C. Cui, W. J. Dong, W. H. Tang and B. Y. Chen, *Mater. Character.* 61, 489 (2010). <http://dx.doi.org/10.1016/j.matchar.2010.01.008>
- [26] T. Wejrzanowski, R. Pielaszek, A. Opalińska, H. Matysiak, W. Lojkowski and K. J. Kurzydowski, *Appl. Surf. Sci.* 253, 204 (2006). <http://dx.doi.org/10.1016/j.apsusc.2006.05.089>
- [27] R. Pielaszek, *Appl. Crystall. Proceedings of the XIX Conference, Krakow, Poland*, 43 (2003).
- [28] T. Özkaya, *Synthesis and magnetic characterization of magnetic nanoparticles. Master Thesis, Fatih University, Istanbul* 2008.
- [29] T. Özkaya, M. S. Toprak, A. Baykal, H. Kavas, Y. Köseoğlu and B. Aktas, *J. Alloy. Compd.* 472, 18 (2009). <http://dx.doi.org/10.1016/j.jallcom.2008.04.101>
- [30] B. Unal, Z. Durmus, H. Kavas, A. Baykal and M. S. Toprak, *Mater. Chem. Phys.* 123, 184 (2010). <http://dx.doi.org/10.1016/j.matchemphys.2010.03.080>
- [31] H. Kavas, Z. Durmus, A. Baykal, A. Aslan, A. Bozkurt and M. S. Toprak, *J. Noncrystall. Solid.* 356, 484 (2010). <http://dx.doi.org/10.1016/j.jnoncrsol.2009.12.022>
- [32] Z. Durmus, H. Kavas, A. Baykal, H. Sozeri L. Alpsoy, S. Ü. C elik and M. S. Toprak, *J. Alloy. Compd.* 509, 2555 (2011). <http://dx.doi.org/10.1016/j.jallcom.2010.11.088>
- [33] Z. Durmus, H. Sözeri, B. Unal , A. Baykal, R. Topkaya, S. Kazan and M. S. Toprak, *Polyhedron* 30, 322 (2011). <http://dx.doi.org/10.1016/j.poly.2010.10.028>
- [34] Z. Durmus, H. Erdemi, A. Aslan , M. S. Toprak and H. Sozeri, *Polyhedron* 30, 419 (2011). <http://dx.doi.org/10.1016/j.poly.2010.11.011>
- [35] Z. Chen and L. Gao, *Mater. Sci. Eng. B* 141, 82 (2007). <http://dx.doi.org/10.1016/j.mseb.2007.06.003>
- [36] Z. Q. Li, Y. J. Xiong and Y. Xie, *Inorg. Chem.* 42, 8105 (2003). <http://dx.doi.org/10.1021/ic034029q>
- [37] H. H. Huang, X. P. Ni, G. L. Loy, C. H. Chew, K. L. Tan, F. C. Loh, J. F. Den and G. Q. Xu, *Langmuir* 12, 909 (1996). <http://dx.doi.org/10.1021/la950435d>
- [38] Y. G. Sun and Y. N. Xia, *Adv. Mater.* 14, 833 (2002). [http://dx.doi.org/10.1002/1521-4095\(20020605\)14:11<833::AID-ADMA833>3.0.CO;2-K](http://dx.doi.org/10.1002/1521-4095(20020605)14:11<833::AID-ADMA833>3.0.CO;2-K)
- [39] J. Dobryszcki and S. Bialozor, *Corros. Sci.* 43, 1309 (2001). [http://dx.doi.org/10.1016/S0010-938X\(00\)00155-4](http://dx.doi.org/10.1016/S0010-938X(00)00155-4)
- [40] X. H. Liu, J. Yang, L. Wang, X. J. Yang and L. D. Lu, *Mater. Sci. Eng. A* 2, 7483 (2003).
- [41] T. Kim and M. Shima, *J. Appl. Phys.* 101, 09M516 (2007).
- [42] Y. Xiaotun, X. Lingge and N. S. Choon, *Hardy CS Nanotechnol.* 14, 62 (2003).
- [43] Z. Durmus, H. Kavas, M. S. Toprak, A. Baykal, T. G. Altzneckic, A. Aslan, A. Bozkurt and S. Cosgun, *J. Alloy. Compd.* 484, 371 (2009). <http://dx.doi.org/10.1016/j.jallcom.2009.04.103>
- [44] B. Ünal, Z. Durmus, A. Baykal, H. Sözeri, M. S. Toprak and L. Alpsoy, *J. Alloy. Compd.* 505, 172 (2010). <http://dx.doi.org/10.1016/j.jallcom.2010.06.022>
- [45] B. D. Cullity, Addison-Wesley, Reading, MA 61, 190 (1972).
- [46] J. Mürbe, A. Rechtenbach and T. Töpfer, *Mater. Chem. Phys.* 110, 426 (2008). <http://dx.doi.org/10.1016/j.matchemphys.2008.02.037>
- [47] R. H. Kodama, A. E. Berkowitz, E. J. McNiff Jr and S. Foner, *Phys. Rev. Lett.* 77, 394 (1996). <http://dx.doi.org/10.1103/PhysRevLett.77.394>
- [48] X. Batlle and A. Labarta, *J. Phys. D Appl. Phys.* 35, 15 (2002). <http://dx.doi.org/10.1088/0022-3727/35/6/201>
- [49] A. E. Berkowitz, J. A. Lahut, I. S. Jacobs, L. M. Levinson and D. W. Forester, *Phys. Rev. Lett.* 34, 594 (1975). <http://dx.doi.org/10.1103/PhysRevLett.34.594>
- [50] C. Kittel, *Introduction to Solid State Physics*, New York, Wiley, 1971.
- [51] K. Uzun, E. Cevik, M. Senel, H. Sozeri, A. Baykal, M. F. Abasyanzk and M. S. Toprak, *J. Nanopart. Res.* 12, 3057 (2010). <http://dx.doi.org/10.1007/s11051-010-9902-9>